

**Design and CFD analysis of centrifugal compressor and turbine for
supercritical CO₂ power cycle**

Ashish Chaudhary

Nabros Energy

Kheda (Gujarat), India.

Email: ne@nabrosenergy.in

Amit Mulchand

Nabros Energy

Kheda (Gujarat), India.

Email: ne@nabrosenergy.in

Punit Dave

Nabros Energy

Kheda (Gujarat), India.

Email: ne@nabrosenergy.in

Vishal Mehta

Nabros Energy

Kheda (Gujarat), India.

Email: ne@nabrosenergy.in

Yagnesh Trivedi

Nabros Energy

Kheda (Gujarat), India.

Email: ne@nabrosenergy.in

Haresh Chauhan

Nabros Energy

Kheda (Gujarat), India.

Email: ne@nabrosenergy.in

Johnny Patel

Nabros Energy

Kheda (Gujarat), India.

Email: ne@nabrosenergy.in

Abstract

Supercritical CO₂ (S-CO₂) power cycles are the most promising technology for high temperature heat sources namely concentrated solar thermal, nuclear, fossil fuel as well as low temperature heat sources like recovered waste heat and geothermal applications. Lower compressibility near critical point (73.8 bar & 31.1 °C) of CO₂ is the main reason.

So far, we have worked on design & CFD analysis of the compressor and turbine for supercritical CO₂. We have developed in house code for meanline design of compressor and turbine considering Aungier's loss correlation in Engineering Equation Solver (EES) for net 10 kWe power generation. Further We have analysed this design using CFD. The operating range of our compressor is 305 K & 75 bar at the inlet side and 320 K & 110 bar at the outlet side. Turbine inlet temperature is 800 K. Fluid properties were implemented via property table in the computational analysis code to simulate nonlinear behaviour near the critical point of CO₂. Hexahedral meshes are generated using ATM optimize technique in ANSYS TurboGrid. Steady state simulation for real gas has been done using k- ω SST turbulence model of Ansys CFX software.

We have achieved 80% isentropic efficiency of turbine and compressor and the compression work has been reduced to 50%, as compared to ideal gas compression process.

Keywords: Turbine, Compressor, CFD, Meanline Design, k- ω SST turbulence model

1. Introduction

Supercritical CO₂ brayton power cycle has gain a lot of attention all over the world after Dostal's thesis publication on the same research topic (Dostal, 2004). Dostal proved that Supercritical CO₂ (S-CO₂) brayton power cycle can reduced 18% percent of cost for power generation compared to steam rankine cycle in Nuclear application. For that, the main reason is the lower compression work and high efficiency at moderately high temperature.

Concentrated solar thermal power (CSP) is an efficient method for producing electrical energy from available non-conventional power generation system. Presently, CSP system is providing 4.7 GW of energy in all over the world. The main challenge in expansion of CSP is high cost per unit power generation compare to solar photovoltaic. The S-CO₂ brayton cycle can increase the overall efficiency of CSP system which may lead to reduction in levelized cost of energy (LCOE). But main challenge in this innovative technology for development at commercialized stage requires stable operation at high pressure environment.

The first CO₂ cycle design was proposed by E. G. Feher in the United States (Feher, 1967). Author demonstrated the need to adopt recuperative configuration to reach high efficiency and discussed the pinch point problem due to variation in thermophysical property above critical condition. Feher (1968) has explained significant advantage of CO₂ as working fluid over other fluid.

- Critical temperature is 31.1 °C, that makes the cooling process above critical point feasible relative to Water ($T_{cr} = 374$ °C).
- It is relatively inexpensive, non-toxic.
- It is inert and stable at the temperature of interest.

Angelino performed one of the most detailed investigations of the supercritical CO₂ cycle. His prime focus was on condensation cycle (Angelino, 1969). He concluded that at turbine inlet temperatures higher than 650 °C single heating CO₂ cycles exhibit a better efficiency (> 50%) than reheat steam cycles.

Department of energy (US) have started sunshot project aiming to reduce the LCOE to 0.06 \$/kWh for CSP technology by 2020 under leadership of Dr. Craig Turchi (Turchi, 2012). Pratt Whitney & Rocketdyne (PWR, California, USA) and Electricite De France (EDF, Paris, France) are studying S-CO₂ cycle design for application to coal power plants (Dowell et al. 2011, Moullec 2012). S-CO₂ power cycle is expected to first be utilized and commercialized for waste heat recovery application. The patents related to this application belong to Echogen (Ohio, USA) and General Electric (New York, USA). Small scale 50 kWe S-CO₂ compression test loop for validation with model employed in turbomachinery and heat exchanger design for Nuclear Application has been developed at Sandia National Laboratory (Wright et al., September 2010). SNL has also developed 30 kWe radial inflow turbine for S-CO₂ (Vilim, August 2011). 18 kWe (gross value) power loop has been demonstrated for 500 K Turbine inlet temperature at Tokyo institute of Technology (Utamura, 2012). Research team concluded after experiment that “Compressor performance in the supercritical liquid like phase achieved highest performance in both experiment and prediction by the simulation program”.

The majority of the work in the literature is on modeling the properties of supercritical fluids (i.e. equation of state (EOS) modeling). The behavior of these fluids in turbomachinery internal flow environments however, is still largely unknown. Current practice employs standard compressor stages designed for conventional fluids for use in supercritical applications. This can lead to decreased performance levels and operability issues. There is unclear description and characterization of the real gas effects of the fluid on the internal flow behavior and related mechanisms to analyze the compressor.

2. Objective

This research work is focused to designing the efficient centrifugal compressor and radial inflow turbine considering real gas behaviour of S-CO₂ working fluid for 30 kWe power generation.

3. Methodology

A) Thermodynamic Analysis of 30 kWe gross power for supercritical CO₂ turbomachinery design

We are investigating advanced brayton power cycle using Supercritical CO₂ as working fluid for CSP application. The schematic layout of the test loops has been shown in figure 1. Inlet pressure of compressor is fixed near to critical point due to fact that compressibility makes liquid like phase and requires lesser work for compression. The pressure drop of 3.5% is taken in the heat addition and rejection process (Garg et al, 2013). Isentropic efficiency of the turbine and compressor are chosen 80% and 75% respectively from the experimental test result of the Sandia National Laboratory (Wright et al, 2010).

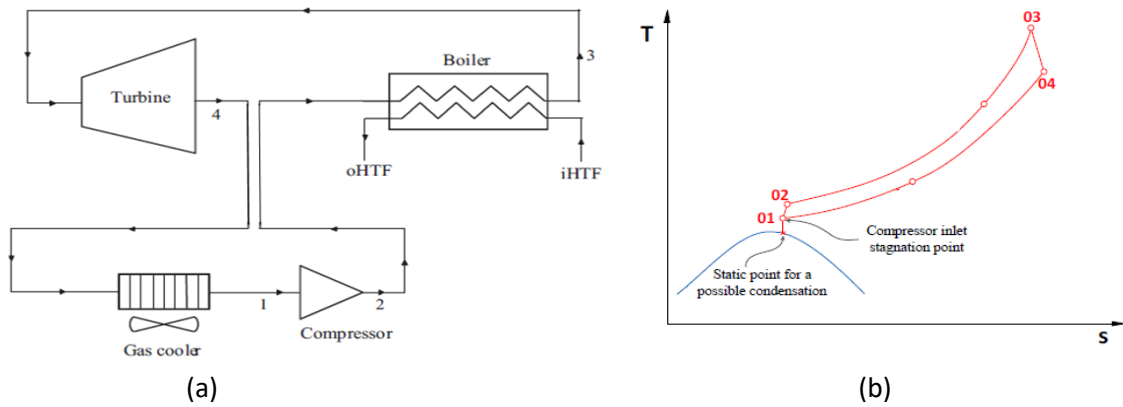


Figure 1: (a) Cycle configuration (b) T-S Diagram

Table 1: Temperature and Pressure at state point

State Points	Pressure (bar)	Temperature (K)	Specific Enthalpy(kJ/kg)	Density (kg/m ³)
1	75	308	396.74	274.97
2	105	331.9	409.27	335.06
3	101.3	800	1014.9	66.185
4	77.72	773.2	985.13	52.819

The mass flow rate for gross work output of 30 kWe is calculated as

$$M_{wf} = \frac{P}{h_3 - h_4} \quad (1)$$

The calculated mass flow rate from above equation is 1.01 kg/s.

B) Meanline Design

i) Compressor: The objective is to find optimum geometry of centrifugal compressor at maximum efficiency by using correlation between specific speed and efficiency. The complete step by step procedure is explained as a flow chart in figure 2. Specific speed is a parameter which relates rpm, volumetric flow rate, and ideal enthalpy rise. There is increase in radius along axial path in centrifugal impeller which delivers higher energy leads to high pressure ratio at single stage.

$$Ns = (\omega * \sqrt{Q})/H_{id}^{3/4} \quad (2)$$

Where,

Ns = Specific speed, ω = RPM, Q = Volumetric flow rate, H_{id} = Ideal enthalpy rise

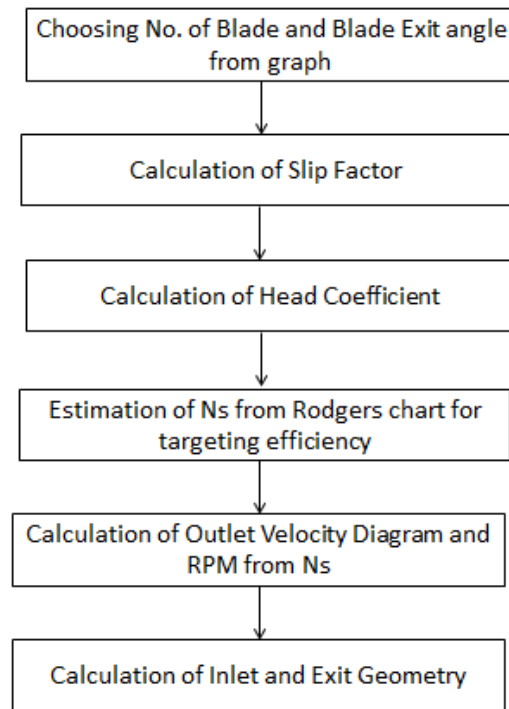


Figure 2: Flow chart for meanline Design

The obtained design from shown flow chart will be validated with result of ANSYS inbuilt module Vista CCD for design. This validation is shown in result and Discussion section.

ii) Turbine: Aungier's method was most appropriate for the meanline analysis. Specific speed is the function of rotational speed, volumetric flow rate at the exit of rotor and ideal enthalpy drop. The total to static efficiency is given by generalized performance chart developed by Aungier. This chart is developed by the two sets of experimental data for radial turbines. This chart (figure 3) is the function of velocity ratio and specific speed.

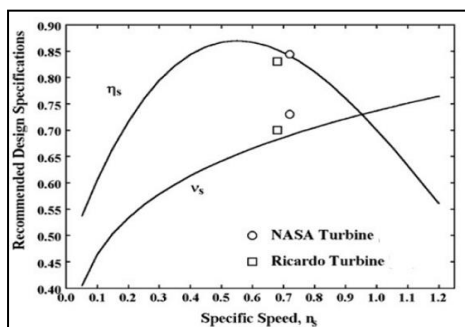


Figure 3: Stage Performance Chart (Aungier, 2005)

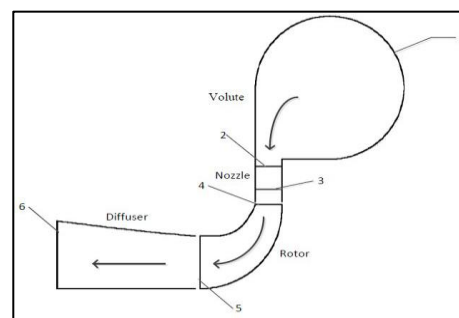


Figure 4: Radial Turbine stage Cross-section (Aungier, 2005)

1 = Volute Inlet Parameter

2 = Volute exit and Nozzle inlet Parameter

3 = Nozzle Exit Parameter

4 = Rotor Inlet Parameter

5 = Rotor Exit Parameter

6 = Diffuser Exit Parameter

As we know the assumed isentropic efficiency, from the graph we can find the value of velocity ratio and specific speed. As shown in figure, velocity ratio is in the range of 0.6-0.7. From the past research

0.68-0.70 is the recommended range for radial turbine. The specific speed value can be finding in the optimum range of 0.4-0.6. The turbine stage can achieve reasonably good performance, due to the fact that generalized correlations are not examined by the practical performance for the working fluid as air.

Once the basic parameters namely velocity ratio and specific speed are available, the rotor inlet velocity triangle and geometry dimensions can be defined. The spouting velocity can be defined by,

$$C_{0s} = \sqrt{2\Delta H_{id}} \quad (3)$$

And the rotor inlet tip velocity is given by:

$$U_4 = v_s C_{0s} \quad (4)$$

As mentioned, the outlet flow is designed for zero swirl at the meanline analysis. The rotor inlet velocity can be find out from the given equation is:

$$C_{u4} = \frac{U_4 \eta_s}{2v_s^2} \quad (5)$$

Rohlik (1968) gave the correlation of inlet absolute angle with function of specific speed as:

$$\alpha_4 = 90 - (10.8 + 14.2n_s^2) \quad (6)$$

Where α_4 is in the degrees that can be find out from the above equation. The inlet Meridional velocity (C_{m4}) can be found out from the below equation:

$$\tan \alpha_4 = \frac{C_{u4}}{C_{m4}} \quad (7)$$

The absolute velocity (C_4), the relative flow angle (β_4) and relative velocity are given by the following equations:

$$C_4 = \sqrt{(C_{u4}^2 + C_{m4}^2)} \quad (8)$$

$$\tan \beta_4 = \frac{W_{u4}}{C_{m4}} \quad (9)$$

$$W_4 = \sqrt{(C_{m4}^2 + W_{u4}^2)} \quad (10)$$

Inlet width of the blade can be found out from the continuity equation.

$$m = \pi D_4 b_4 \rho_4 C_{m4} \quad (11)$$

Thus, the inlet velocity triangle and the main geometry dimensions can be determined from the above parameters. The rotor exit velocity triangle can be found out from the conventional coefficient which are discussed and recommended by the Aungier. The ratio of meridional velocity ratio is:

$$\frac{C_{m5}}{C_{m4}} = 1 + 5 \left(\frac{b_4}{r_4} \right)^2 \quad (12)$$

The ratio of $\frac{C_{m5}}{C_{m4}}$ should be lies between $1 < \left(\frac{C_{m5}}{C_{m4}}\right) < 1.5$ (Wood, 1963).

The stage flow coefficient and head coefficient can be calculated as well and that should be in the recommended range which shown in the figure 5 is given by Chen and Baines (1994). This graph shows contour of blade loading and flow coefficient to the total to static efficiency.

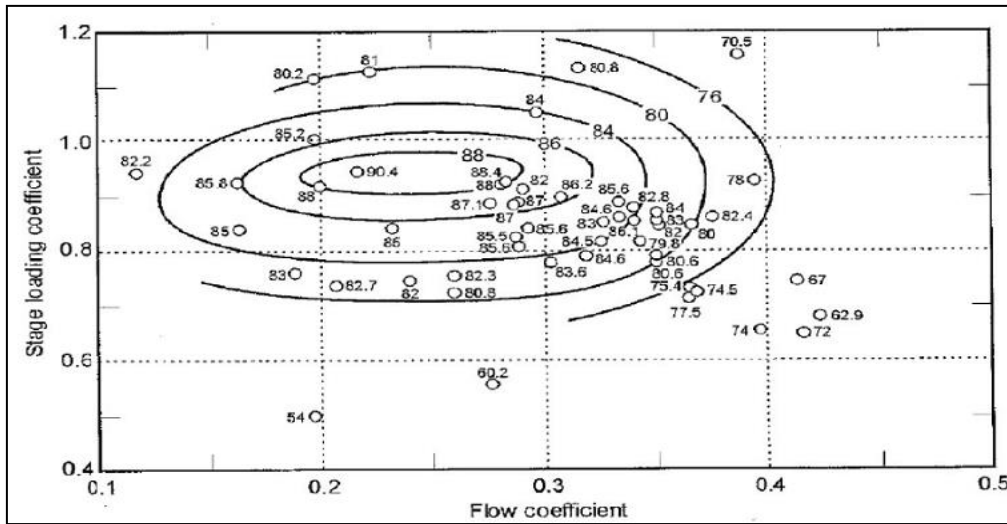


Figure 5:- Correlation of stage loading and head coefficient shows total to static efficiency

From the graph shows that the value of stage loading coefficient (ψ) lies between 0.8-1.0 and flow coefficient (ϕ) should be lies between 0.2-0.3. The contour of total to static efficiency indicate that a reasonable value. The values should be lies between the optimum range.

$$\phi = \frac{C_{m5}}{U_4} \quad (12)$$

$$\psi = \frac{C_{u4}}{U_4} \quad (13)$$

If the corresponding efficiency lies with the optimum area, it suggests that preliminary design is appropriate and reasonable for radial inflow turbine.

After that rotor inlet leading edge thickness recommended by Aungier (2005).

$$t_{leading} = 0.04r_4 \quad (14)$$

The ratio of outlet hub radius (r_{h5}) and inlet radius of impeller (r_4) IS 0.3 which was recommended by Baines (2003).

$$r_{h5} = 0.3r_4 \quad (15)$$

Rotor trailing edge thickness can be found from the Aungier's equation:

$$t_{trailing} = 0.02r_4 \quad (16)$$

Shroud radius (r_{s5}) at the rotor outlet:

$$r_{s5} = \sqrt{\frac{A_5}{\Pi} + (r_{h5})^2} \quad (17)$$

In the Eq 4.19, the rotor outlet area can be found from the mass conservation equation:

$$A_5 = \frac{m}{\rho_5 C_{m5}} \quad (18)$$

Rotor outlet blade width:

$$b_5 = r_{s5} - r_{h5} \quad (19)$$

Mean radius at rotor outlet:

$$r_5 = \frac{(r_{h5} + r_{s5})}{2} \quad (20)$$

Blade speed at rotor outlet:

$$U_5 = r_5 \omega \quad (21)$$

Meridional component of relative velocity at rotor outlet:

$$W_{m5} = C_{m5} \quad (22)$$

In that way, we can find outlet velocity triangle and their required geometry. This coding was developed in the EES software, so we only required input parameters namely total temperature, total pressure, mass flow rate and gross power is required. By using these parameters, we can find the geometry regarding to conditions.

From the above discussion, the fundamental performance parameters like head coefficient, flow coefficient, specific speed should be in recommended range. Hence, we can find optimum and efficient turbine geometry.

i) Selection of Number of Rotor Blades

The number of blades is function of stator exit absolute angle which is given by different authors. It is observed that minimum number of blades given by Whitfield [13] and Glassman et al (1976) Correlation which is very suitable for small Radial inflow turbine.

Glassman (1976) equation is:

$$N_r = \left(\frac{\Pi}{30}\right) (110 - \alpha_4) \tan \alpha_4 \quad (23)$$

Where α_4 is in degrees and it is suitable for small radial inflow turbine which are used in Supercritical CO₂ plants.

C) CFD Analysis for Compressor

The data from meanline design is then exported to Bladegen. Bladegen is an inbuilt module in Ansys for generating three-dimensional structure of turbomachinery. 3D impeller geometry can be obtained from 1D design as shown in figure 6.

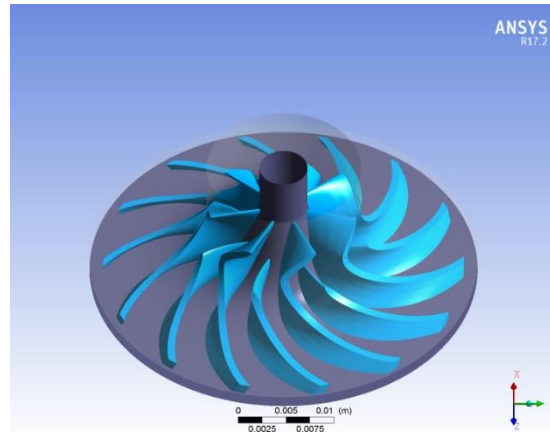


Figure 6: Three dimensional CAD model

Thermal property of S-CO₂ is highly nonlinear near critical point which shows it doesn't follow ideal gas rule. To simulate nonlinear behavior near the critical point of CO₂, the fluid properties were implemented, via property table, in the computational analysis code. Real gas property is provided by the NIST Refprop based on Span and Wagner equation of state in the form of .RGP extension file. This RGP file can be import through User Defined Material in CFX. After defining gas property, boundary conditions are required to set up for simulation in which one has to choose turbulence model. Fluid is turbulence in most of turbomachinery due to high Reynolds number. However, Reynolds number still increases further in S-CO₂ due to its high density.

Ansys provides inbuilt module of Turbogrid which generates high quality hexahedral meshes for three dimensional fluid flow analyses. Three dimensional design from Bladegen is then imported to Turbogrid for meshing. Shroud tip gap is provided in mm. A global size factor set 1 called as "Fine mesh" around 380000 cells without boundary layer. Then calculated Reynolds number from 1D design is employed by the software to calculate the distribution of boundary layer mesh. Boundary layer refinement can be done using cut-off edge to boundary layer factor. Near wall element size is fixed as y+ offset from calculated Reynolds Number. Main objective of y+ method is to set value for first layer of node to relative value of y+ in relation to Reynolds number. Completing all necessary tasks, finally 3D meshes are generated with total number of element 625100 and total number of nodes 678000. (as shown in figure 7)

Table 2: Parameter considered in Meshing

General Parameter	
Reynolds Number	5*10 ⁷
Shroud Tip mesh Method	Match Expansion at Blade Tip
Topology Mesh Technique	ATM optimized
Boundary Layer Refinement Control Factor	Proportional to Mesh Size
Near Wall Treatment	Y+ Method

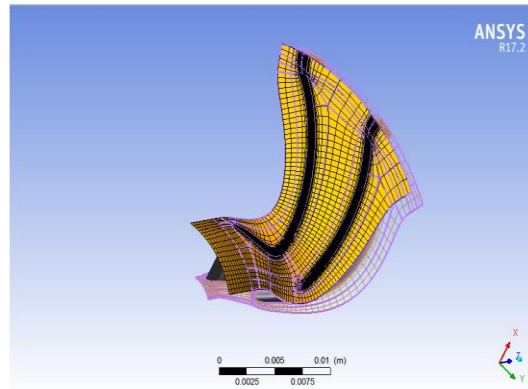


Figure 7: Single passage Meshing

Ansys CFX provides the two models for turbulence namely: $k-\omega$ Shear stress model and $k-\epsilon$ model. Wilcox initially proposed the $k-\omega$ model in 1988 (Wilcox, 1988). Menter had modified further changed to $k-\omega$ Shear stress model (Menter, 1994). $k-\epsilon$ model was proposed by Launder and Spalding in 1972 means older than $k-\omega$. This model is suitable for fully turbulent non-separated flows. It does not calculate very accurate flow field that exhibit adverse pressure gradient and strong curvature. Problem related to external body can be simulated more accurately with $k-\epsilon$ model. $k-\omega$ shear stress model (SST) is recommended for accurate simulation in near wall treatment and internal flow like turbomachinery (Pecnik et al., 2012). SST model is chosen for the steady state flow simulation in S-CO₂ compressor.

Total pressure and temperature are defined at inlet with mass flow rate at outlet as boundary condition shown in figure 8.

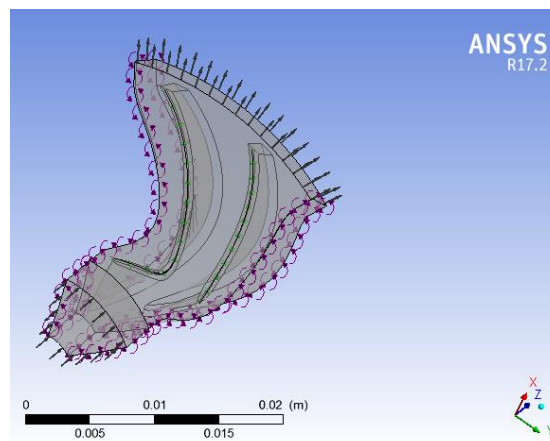


Figure 8: Boundary Condition

4. Result and Discussion

a) Compressor

3 D numerical simulation is done considering the real gas behavior, the obtained results were compared a with meanline analysis. Overall result indicated the power required for compression is getting reduced up to 50% for real fluid compared to ideal fluid. The main reason for obtaining this result can be explained from following condition.

- S-CO₂ has a density of 300 kg/m³ at inlet of compressor which is 30% of liquid water density.
- The compressibility factor is about 0.4 which makes fluid more liquid like nature.
- The diffuser and inlet guide vanes (IGV) are excluded in this work. In rotodynamic, many losses are associated with stator component like IGV and diffuser

Table 3: Comparison of meanline design with Ansys Vista CCD result for centrifugal compressor

Method	D ₂ in m	D _{tip} in m	D _{hub} in m	β ₁ in degree	Exit Width Gap (mm)
Mean Line	0.03745	0.01947	0.0058	51.79	0.9
Ansys	0.03916	0.019	0.0055	47.4	1
Deviation	4.5 %	2.41 %	5.17%	8.47 %	10 %

Table 4: Comparison thermodynamic property

Property	Location	Analysis Type	
		Meanline Design	Real Gas (CFD)
T _{static} in K	In	307	307.2
	Out	326.7	318
T _{total} in K	In	308	308
	Out	338	324
P _{static} in bar	In	72	74
	Out	88	95
P _{total} in bar	In	75	75
	Out	105	105
Density in Kg/m ³	In	129	271.14
	Out	146	418.5

Table 5: Performance comparison

Parameter	Meanline Design	CFD
Isentropic efficiency	83 %	80%
Power Consumption	25 kW	12 kW

Total and static temperature variations for both cases are shown in figure 9. Graph clearly indicated that temperature increment is higher in ideal case, means more isentropic work needed for compression. The slope of total temperature is higher than static temperature that shows the kinetic energy is also increasing due to centrifugal effect in the channel path.

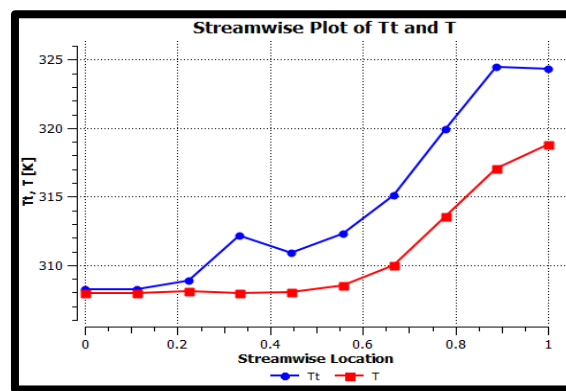


Figure 9: Temperature Variation in Compressor for real fluid

Total pressure and static pressure variation along meridional path are shown in figure 10 for both cases. Graph shows the pressure is increasing due to compression in the impeller under aerodynamic and centrifugal force. Static pressure is less at exit for ideal compare to real fluid but total pressure are approximately same that indicates the pressure loss are more in the case of ideal. Slope is high for total pressure with respect to static pressure, the reason is same that velocity is increased along the meridional channel. Blade height is decreasing continuously along the channel that also increases the kinetic energy of fluid.

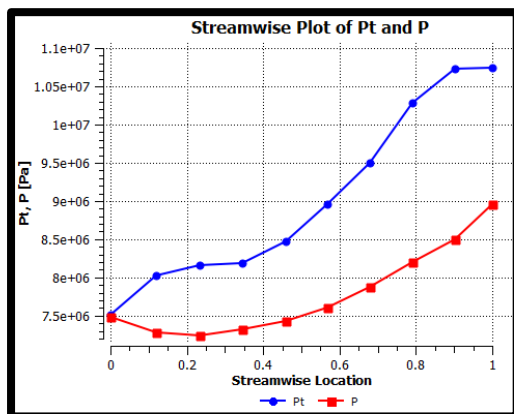


Figure 10: Pressure variation in compressor for real fluid

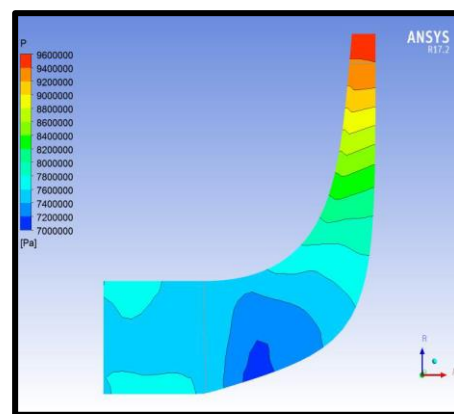


Figure 11: Static Pressure Contour on passage

b) Turbine: From the discussion of the meanline design, in house code is generated in the EES software. The result are discussed namely inlet and outlet velocity triangle at the rotor inlet and outlet.

Table 6: Velocity triangle at inlet and outlet

Parameter	Value (m/s)		Parameter	Value (m/s)
U_4	193.1		U_5	88.71
C_4	177.4		C_5	46.03
W_4	46.78		W_5	99.94
U_{H5}	57.93		N	86837 (rpm)
U_{S5}	119.5		C_0	279.9

The performance parameters which are consider during the design consideration. Head coefficient, flow coefficient, specific speed, and velocity ratio are in the recommended range which is suggested by the Aungier.

Table 7: Performance Parameter

Performance Parameters	Recommended Range	Result
Head Coefficient	0.8-1.0	0.8927
Flow Coefficient	0.2-0.4	0.2484
Velocity Ratio	0.6-0.7	0.69 (Fixed)
Specific Speed	0.4-0.6	0.45 (Fixed)
Meridional Speed Ratio	1-1.5	1.09
Stage Reaction	0.45-0.65	0.53

Hence, from the above discussion, the velocity triangle and performance parameters, we can find the geometry of the turbine at the design point.

Table 8: Obtained Geometry

Geometry	Value	Geometry	Value
D_4	42.49 (mm)	D_{H5}	12.75 (mm)
b_4	2.96 (mm)	D_{S5}	26.29 (mm)
α_4 (Flow Angle)	76.32 (Degree)	α_5	0 (degree)
β_4 (Flow Angle)	-26.3 (Degree)	β_5	-62.58 (mm)
ϵ_r	0.0005 (mm)	N_r (Blades)	15
$T_{trailinge}$	0.4249 (mm)	$T_{leading}$	0.8489 (mm)
Z_r	10.16 (mm)	b_5	6.773 (mm)

Table 9: Comparison of Thermodynamic Property

Property	Location	Analysis Type	
		Mean Line (Analytical)	Real Gas (CFD)
T_{static} In K	In	800	800
	Out	768.5	769.5
T_{total} In K	In	800	800
	Out	770.5	771.4
P_{static} In bar	In	101.30	101.30
	Out	77.36	76.50
P_{total} In bar	In	101.30	101.30
	Out	77.92	76.98
Density In kg/m³	In	60.87	62.5
	Out	52.86	53

The expansion of the pressure at the inlet is 101.30 bar to expanded up to 77 bar which is shown in the figure 12 in pressure contour. The inlet of the blade, density is 65 kg/m³ and because of expansion the outlet density is become 51 kg/m³.

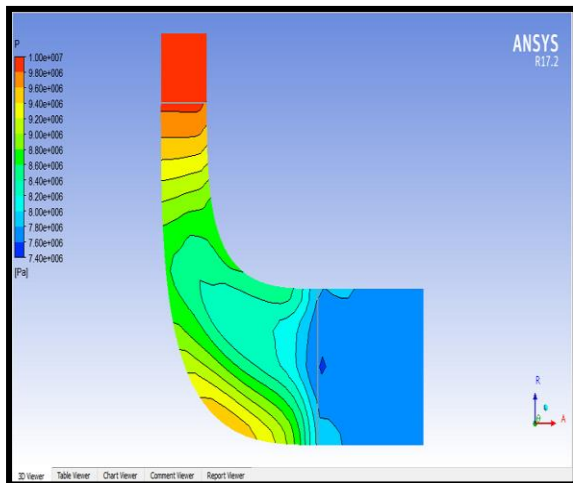


Figure 12: Pressure contour of Meridional view in radial turbine

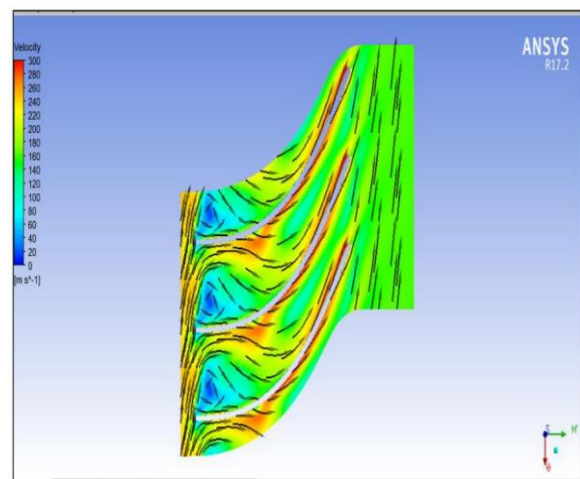


Figure 13: velocity contour at span of 50% of blade

After second point flow enters to the blade of expansion wheel where it loses its kinetic energy by giving mechanical work. Because of extraction of work velocity of a gas is constantly reduce which is shown in Figure 13.

5. Conclusion

Present work has been carried for development of 30 kW S-CO₂ turbomachinery experimental set up for concentrated solar power application. All transport properties of CO₂ are highly non-linear near critical point, finding the effect of this behaviour on the compressor performance. The size of impeller is very small because of high density (nearly about 30% of water density) at inlet of compressor that leads to very high RPM of about 60000. The meanline analysis results are validated with CFD result. Inlet hub shroud diameter and exit diameter are compared with CFD result and found that results deviated by 5%, 2.41% and 4.17%.

Analysis was carried out for real and ideal gas separately. It is found that the power for compression is reduced 50% for real gas compared to ideal gas compression under the effect of compressibility factor which is 0.3 near to liquid nature. Here, isentropic efficiency is produced near about 80% for CFD while according meanline analysis shows 83% efficiency of S-CO₂ compressor. At the end of compression, the difference between density is very high between this two cases and the reason is nonlinear thermophysical properties of supercritical CO₂

near critical point. It is further concluded that there is much difference between result obtained in ideal and real gas, CO₂ follows liquid like nature at 75 bar pressure and 308 K temperature. So, it is recommended to use real gas model for further simulation.

From the meanline design in Turbine, the incidence inlet angle is -26.3o degree which is in recommended range for the optimum angle between -20o to -40o. The maximum Mach number is 0.4 at the inlet of the absolute velocity. So there is no hint to indicate that choking occurs during the turbine work. The value of Stage coefficient and Flow coefficient are 0.2384 ($0.2 < \Phi < 0.4$) and 0.8927 ($0.8 < \Psi < 1.0$). Overall efficiency is 80 % shown in result.

6. References

1. Angelino, G., 1968, "Carbon Dioxide Condensation Cycles for Power Production," *Journal of Engineering for Power*, 10, July, pp. 287-295
2. Benjamin Monje et al., 2014, "A DESIGN STRATEGY FOR SUPERCRITICAL CO₂ COMPRESSORS" ASME Turbo Expo 2014 GT2014 June 16 – 20, 2014
3. Dostal, V. & Kulhanec, M., 2009. Research on the Supercritical Carbon Dioxide Cycles in the Czech Republic. Troy, New York (US), Proceedings of the SCO₂ Power Cycle Symposium 2009
4. E. Feher, "The supercritical thermodynamic power cycle," *Energy Conversion*, Vol. 8, pp. 85-90. Pergamon Press, 1968.
5. Garg Pardeep and Pramod kumar, 2013, "Supercritical CO₂ brayton power cycle for solar thermal power generation" *J. of Supercritical Fluids* 76 (2013) 54– 60
6. G. Kimzey, Development of a Brayton Bottoming Cycle Using Supercritical Carbon Dioxide as the Working Fluid, Electric Power Research Institute Report, Palo Alto (CA), 2012
7. Haghshenas Fard M, Hooman K, Chua H. Numerical simulation of a supercritical CO₂ geo thermo siphon. *International Communications in Heat and Mass Transfer* 37, 6pp. 1447-1451, 2010
8. H. Yamaguchi , X.R. Zhang , K. Fujima , M. Enomoto , N. Sawada, 2006, Solar energy powered Rankine cycle using supercritical CO₂, *Applied Thermal Engineering* 26 (2006) 2345–2354
9. NREL, 2012. 10-Megawatt Supercritical Carbon Dioxide Turbine Test-Thermodynamic Cycle to Revolutionize CSP. http://www.nrel.gov/csp/supercritical_co2.html
10. Rene Pecnik, Enrico Rinaldi, Piero Colonna, 2013, "Steady State CFD Investigation of a Radial Compressor Operating with Supercritical CO₂," ASME Paper No. GT2013-94580, Antonia, USA
11. Steven A. Wright, Paul S. Pickard, Ross F. Radel, Milton E. Vernon, Robert Fuller, 2009, "Supercritical CO₂ Brayton Cycle Power Generation Development Program and Initial Test Results," ASME Paper POWER2009-81081, Albuquerque, New Mexico, USA
12. Aungier, R. H., (2005), "Turbine Aerodynamics: Axial-Flow and Radial-Inflow Turbine Design and Analysis," The American Society of Mechanical Engineers Press, New York